The Effect of Subtropical Cooling on the Amplitude of ENSO: A Numerical Study

DE-ZHENG SUN, TAO ZHANG, AND SANG-IK SHIN

NOAA–CIRES Climate Diagnostics Center, Boulder, Colorado

(Manuscript received 28 April 2003, in final form 31 March 2004)

ABSTRACT

The effect of an enhanced subtropical surface cooling on El Niño–Southern Oscillation (ENSO) through the ''ocean tunnel'' is investigated using a coupled model. Here, the term ''ocean tunnel'' refers to the water pathway that connects the equatorial upwelling water to the subtropical/extratropical surface water. The subtropical cooling is introduced through a reduction of the radiative–convective equilibrium SST (SST_p) in that region. The SST_p for the equatorial region is kept fixed.

It is found that an enhanced cooling in the subtropics results in a regime with stronger ENSO. This is because an enhanced subtropical cooling reduces the temperature of the water feeding the equatorial undercurrent through the ocean tunnel. The resulting larger difference between the warm-pool SST and the temperature of the equatorial thermocline water—the source water for the equatorial upwelling—tends to increase the equatorial zonal SST contrast between the western and the eastern Pacific. In response to this destabilizing forcing to the coupled equatorial ocean–atmosphere, a stronger ENSO develops. ENSO is found to regulate the time-mean difference between the warm-pool SST and the temperature of the equatorial undercurrent. The findings provide further support for the ''heat pump'' hypothesis for ENSO, which states that ENSO is an instability driven by the meridional differential heating over the Pacific Ocean and that ENSO regulates the long-term stability of the coupled equatorial Pacific climate. The results also substantiate the notion that surface variability from higher latitudes may influence equatorial SST variability through the ocean tunnel.

1. Introduction

The effect of El Niño–Southern Oscillation (ENSO) on the subtropical/extratropical climate has been extensively studied and is well understood (see review by Trenberth et al. 1998 and by Alexander et al. 2002). In contrast, our understanding of the influence of subtropical/extratropical climate on ENSO is very limited. This study is motivated to improve this situation, specifically by addressing the question of how ENSO amplitude may respond to an enhanced subtropical cooling over the Pacific Ocean.

A significant role of the subtropical cooling in modulating the amplitude of ENSO has been hinted by the finding of an ''ocean tunnel''—the water constituting the equatorial undercurrent and therefore the upwelling water in the equatorial Pacific that comes from the subtropical/extratropical region (Pedlosky 1987; Liu et al. 1994; McCreary and Lu 1994). Gu and Philander (1997) even hypothesized that such a ''tunnel'' may be an underlying cause for the Pacific decadal variability. Zhang et al. (1998) provided further observational support for this hypothesis. Although it is found later that the processes in the real ocean appear to be more complex than what Gu and Philander (1997) originally envisioned (Lu et al. 1998; Schneider et al. 1999), the finding remains robust that the water feeding the equatorial undercurrent comes from the subtropics. Using two ocean GCMs, Shin and Liu (2000) demonstrated that a change in the subtropical/extratropical SST could induce a significant change in the temperature of the equatorial thermocline. Unfortunately, in their perturbation experiments, the equatorial winds are not coupled to the SST, effectively eliminating a necessary mechanism supporting ENSO. Nonetheless, their results add weight to the possibility of a significant subtropical/extratropical impact on ENSO through the aforementioned ocean tunnel. It has been known since the pioneering study of Zebiak and Cane (1987) that El Niño results from instability of the coupled tropical ocean–atmosphere (see also the review by Neelin et al. 1998). A change in the equatorial thermocline temperature is an effective way to perturb the stability of the equatorial ocean. For example, a colder equatorial undercurrent would result in colder upwelling water in the eastern equatorial Pacific. The subsequent cooling on the SST in the eastern equatorial Pacific then strengthens the equatorial zonal SST contrast between the western and eastern Pacific, which may render the coupled equatorial Pacific system less stable, triggering the onset of a regime with stronger ENSO.

The need to examine the response of ENSO to an

Corresponding author address: Dr. De-Zheng Sun, NOAA–CIRES Climate Diagnostics Center, 325 Broadway, Boulder, CO 80304.
E-mail: dezheng.sun@noaa.gov

enhanced subtropical/extratropical cooling is further highlighted by the ''heat pump'' hypothesis for ENSO (Sun 2003). Based on an analysis of the heat balance in the equatorial Pacific, Sun has suggested that the amplitude of ENSO may be linked to the poleward heat transport out of the equatorial ocean and therefore by extension to the meridional differential heating over the Pacific Ocean. Sun (2003) has conducted further numerical experiments demonstrating that an increase in the equatorial surface heating (or equivalently an increase in the tropical maximum SST) results in a regime with more energetic ENSO. Specifically, Sun has found that an increase in the radiative heating over the equatorial region increases the difference between the tropical maximum SST—the warm-pool SST—and the temperature of the equatorial thermocline water. This further tends to increase the equatorial zonal SST contrast. Stronger ENSO develops to counteract this tendency. The difference between the warm-pool SST and the temperature of the equatorial thermocline water may also be increased by a cooling of the equatorial undercurrent. We expect that an enhanced subtropical/extratropical cooling will induce a cooling to the equatorial undercurrent via the aforementioned ocean tunnel.

2. Methods

This study therefore aims to extend the study of Sun (2003) and to further explore the concept that ENSO is driven by the meridional surface differential heating over the Pacific. The same numerical model used in that study will be used to investigate the effect of a cooling over the subtropical Pacific on the amplitude of ENSO. The atmospheric component of the coupled model of Sun (2003) is an empirical atmospheric model. The surface heat flux into the ocean is assumed to be proportional to the difference between the radiative–convective equilibrium SST (SST_p) and the actual SST,

$$F_s(\lambda, \phi) = C_p \rho c H_m [\mathrm{SST}_p(\phi) - \mathrm{SST}(\lambda, \varphi)], \quad (1)$$

where F_s is the net surface heat flux into the ocean, λ is the longitude, ϕ is the latitude, C_p is the specific heat, ρ is the density, c is the restoring coefficient, and H_m is the depth of the mixed layer (50 m). The SST_p in the equation is prescribed empirically such that the model ocean is heated in the equatorial region and cooled in the higher latitudes [see Eq. (5) in Sun (2003) for the exact form of the prescribed SST_p]. The restoring coefficient c is estimated from observations (5.8×10^{-8} s^{-1}; Sun 2003). Over the equatorial region, the zonal wind is coupled to the zonal SST gradients in the following form,

$$\tau^x(\lambda, \phi) = \tau^x_{\mathrm{ref}}(\lambda, \phi) - \mu(\phi)(\Delta T - \Delta T_{\mathrm{ref}}), \quad (2)$$

where τ^x is the zonal wind stress, and τ^x_{ref} is the zonal wind stress that is used to spin up the ocean model to obtain a reference state. The climatological annual mean wind stress from the National Centers for Environmental Prediction (NCEP) reanalysis for the period of 1980–99 was used as τ^x_{ref}. A measure of the equatorial zonal SST contrast of the reference state is denoted by ΔT_{ref}. It is defined as the area-averaged SST difference between (5°S–5°N, 130°E–180°) and (5°S–5°N, 230°–280°E). The same measure of the actual equatorial zonal SST contrast predicted by the model is denoted by ΔT. Here μ measures the coupling strength and has a prescribed meridional profile—it decreases away from the equatorial region following a cosine profile. Outside the region of 15°S–15°N, the influence of the equatorial zonal SST contrast on the winds is assumed to be negligible. The value of μ at the equator, taken as 0.0060 $\mathrm{N\ m^{-2}\ K^{-1}}$, is assessed from the observed interannual variations of zonal winds (NCEP winds) and the zonal SST contrast. For example, by linearly regressing the monthly mean interannual anomalies of the NCEP zonal wind stress (Kalnay et al. 1996) in the central equatorial Pacific (5°S–5°N, 160°–200°E) over the period 1980–2002 to the corresponding variations in the equatorial zonal SST contrast (ΔT) (Rayner et al. 1996), one obtains a regression coefficient of $0.0059 \pm 0.000\,53$ $\mathrm{N\ m^{-2}\ K^{-1}}$.

The ocean component is the National Center for Atmospheric Research (NCAR) Pacific basin model (Gent and Cane 1989; Gent 1991). The ocean model is a primitive equation model for the equatorial upper ocean. It employs the reduced gravity assumption so that the deep ocean is at rest. The model consists of a mixed layer and an active layer below which is further divided into six numerical layers by means of sigma coordinates. The temperature of each layer is calculated from its corresponding thermodynamic equation. Therefore, different from the model of Zebiak and Cane (1987), the present ocean model explicitly calculates the heat budget of the entire upper ocean. The model has a 1° resolution in the longitudinal direction and a variable resolution in the meridional direction. Within the equatorial waveguide, the resolution is as fine as 0.25°, thus ensuring accurate simulation of the equatorial waves and the associated dynamic adjustment.

Enhanced cooling in the subtropical ocean is introduced by reducing SST_p in that region. The dynamical coupling between the atmosphere and ocean in the coupled model is at present limited to the equatorial region. Coupling between the winds and the SST in the equatorial region is a necessary mechanism supporting ENSO (Zebiak and Cane 1987; Jin 1996; Neelin et al. 1998). The goal of the present effort is to investigate whether a cooling in the subtropical ocean can affect the amplitude of ENSO through the ocean tunnel that connects the surface ocean in the subtropical region with the subsurface ocean in the equatorial region (Pedlosky 1987; Liu et al. 1994; McCreary and Lu 1994).

3. Results

Figure 1a shows the time series of Niño-3 SST from a control run and a perturbed run. The perturbed run

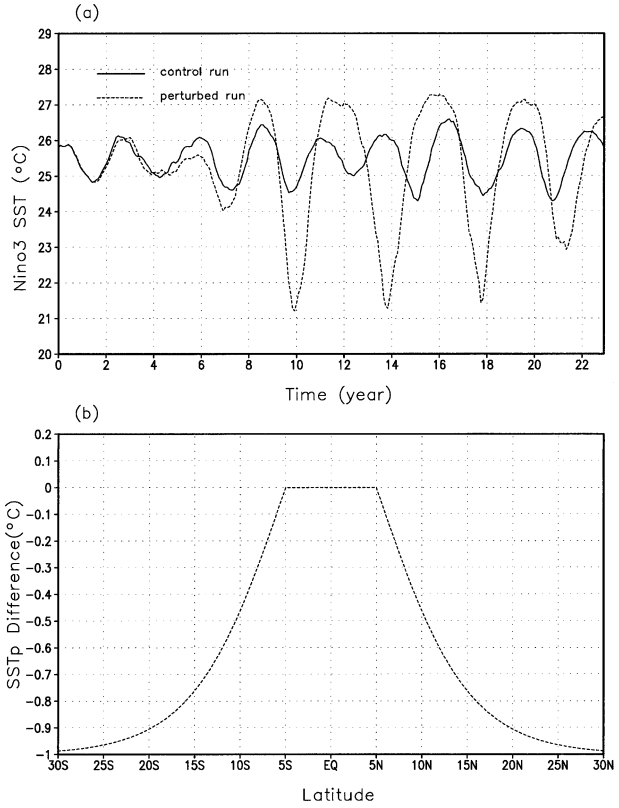

FIG. 1. (a) Time series of Niño-3 SST from the control run (solid line) and the perturbed run (dashed line). The two runs start from the same initial condition. (b) The reduction in SST_p the perturbed run is subjected to.

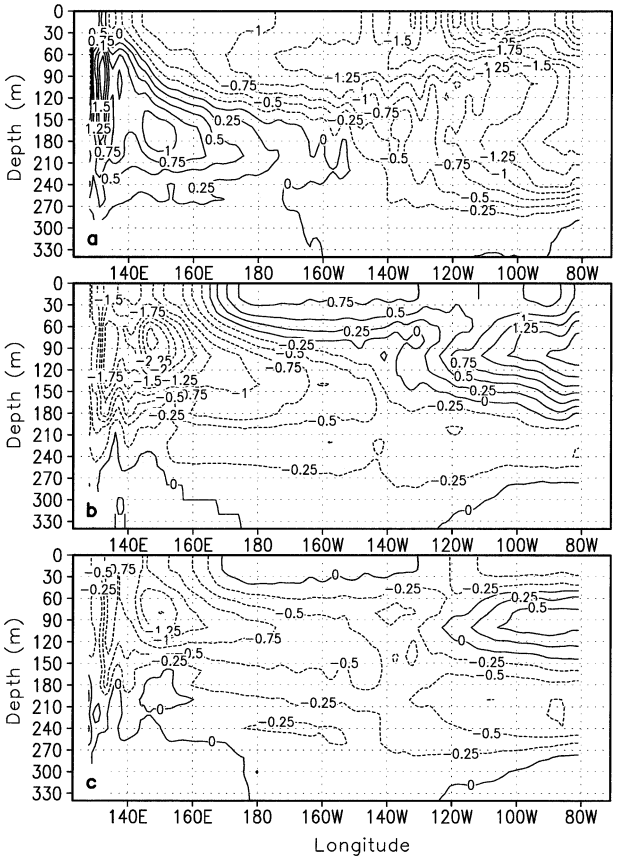

FIG. 2. The differences in the equatorial upper-ocean temperature (5°S–5°N) between the coupled control run and the coupled perturbed run (perturbed run minus control run) in the (a) cold phase, (b) warm phase, and (c) time mean. The definitions of the warm and cold phases are the same as in Sun (2003). The last 16 yr of the run shown in Fig. 1a are used in this calculation.

has an enhanced cooling in the subtropical ocean. The exact difference between the SST_p in the control run and the perturbed run is shown in Fig. 1b. To be in line with the heating experiment reported in Sun (2003), the enhanced cooling starts from the off-equatorial region and is assumed to increase with the latitude. The maximum cooling is reached at the poleward boundary of the ocean model: 30°S and 30°N. The working hypothesis is that enhanced subtropical/extratropical cooling affects the amplitude of ENSO through its effect on the temperature of the equatorial undercurrent (Sun 2000, 2003). Therefore, we are here simply seeking a cooling that will induce significant reduction in the temperature of the equatorial thermocline water. As we will see, such a form of cooling does cool the equatorial undercurrent significantly.

The two runs shown in Fig. 1a start from the same initial condition. After some years of delay (about 8 yr in this particular case), stronger ENSO develops. Note that La Niña becomes colder and El Niño become warmer. Comparing with the amount of cooling introduced outside of the equatorial region, the change in the amplitude of ENSO appears to be large. We will return to this sensitivity issue later. Figure 2 further shows the differences in the equatorial upper-ocean temperature between the control run and the perturbed run during La Niña, El Niño, and in the time mean. The subsurface temperature differences during La Niña and El Niño have a similar pattern to the corresponding temperature anomalies in the control run (Figs. 3a,b). The subsurface signatures of ENSO in both the western and the eastern Pacific are amplified by the imposed subtropical surface cooling. Therefore, we here present a good example showing how an external thermal forcing projects its impact on the internal mode of the system. The impact of this cooling on the time-mean state is much subdued, compared to the impact on the temperature structure during the two phases of ENSO.

The response of ENSO amplitude to the imposed subtropical cooling may be understood by first checking the effect of the subtropical cooling on the stability of the equatorial Pacific ocean–atmosphere. To this end, we have run the same experiments shown in Fig. 1, but without the coupling between the equatorial surface winds and the equatorial zonal SST gradients. Therefore, the feedback from the coupled instability—ENSO—is artificially suppressed. Figure 4a compares

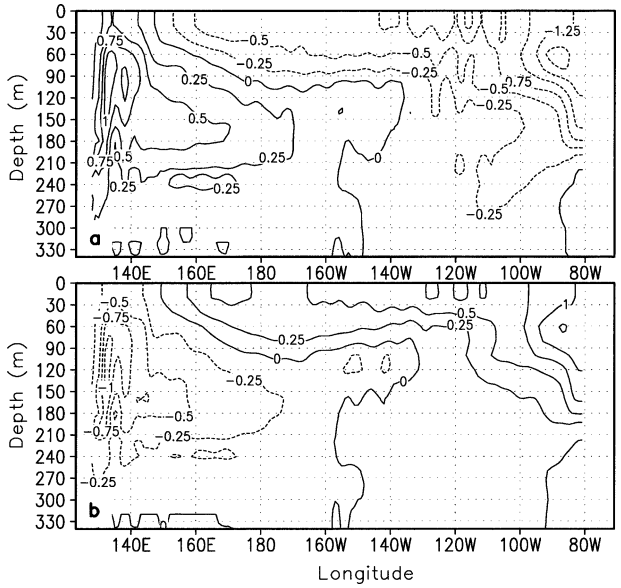

FIG. 3. The equatorial upper-ocean temperature anomalies during the (a) cold phase and (b) warm phase of the control run whose Niño-3 SST is shown in Fig. 1a.

the value of the temperature of the equatorial undercurrent (T_c) from the control experiment with that from the perturbed experiment as a function of time. Here T_c is defined as the zonal mean core temperature of the equatorial undercurrent. It is obtained by first finding the equatorial ocean temperature at the depth where the zonal velocity has its maximum value and then averaging this temperature across the region of 180°—270°E; T_c is meant to be a simple measure of the characteristic temperature of the equatorial thermocline water. Figure 4a shows that the value of T_c from the perturbed experiment with enhanced subtropical cooling starts to diverge from the corresponding value of T_c from the control run after a few years. Figures 4b and 4c further show the meridional cross sections in the central (160°–210°E) and the eastern Pacific (210°–270°E) of the upper-ocean temperature differences between the control run and the perturbation run. The surface cooling in the subtropical ocean clearly sinks into the equatorial thermocline. As a consequence, the equatorial thermocline water is about 1°C colder across the entire equatorial Pacific (Fig. 5). The temperature anomaly in the equatorial thermocline is even larger than the surface cooling imposed in the subtropics. This amplification may have something to do with propagation of Rossby waves originating from the forcing region into the baroclinically unstable regions in the lower limb of the subtropical gyre. Note that in this model, there is no salinity. The temperature perturbations are also density perturbations. Liu and Shin (1999) show that the subduction of density anomalies in their model may be explained as propagation of baroclinic Rossby waves. Galanti and Tziperman (2003) suggest that the equatorward-propagating Rossby waves could be amplified in passing through the baroclinically unstable regions in the lower limb of the subtropical gyre.

Without the equatorial ocean–atmosphere coupling, the 1°C or so cooling to the thermocline water causes little change in the SST of the western Pacific warm pool (Fig. 5). The mean SST over the equatorial western Pacific warm-pool region (5°S–5°N, 120°–160°E)—we here use T_w to represent this temperature—is reduced only by 0.04°C. Two factors apparently prevent significant cooling to the warm-pool SST. One is the considerable depth of the thermocline in the western Pacific. The other is the fact the radiative–convective equilibrium SST (SST_p) is kept fixed for the equatorial region (Fig. 1b). Therefore, the imposed subtropical cooling increases considerably the difference between the warm-pool SST and the temperature of the equatorial thermocline water (the value of $T_w - T_c$ is increased by about 1°C).

The difference between T_w and T_c is a key parameter determining the stability of the coupled equatorial ocean–atmosphere system. The larger the difference between T_w and T_c, the less stable the coupled system (Sun and Liu 1996; Sun 1997). This is because the value of $T_w - T_c$ affects the zonal SST contrast and thereby the zonal wind stress. A positive perturbation to the equatorial zonal SST contrast is evident in Fig. 5. The shallower thermocline in the central and eastern Pacific apparently allows the colder equatorial upwelling water to cool the SST in that region more effectively than it does to the western Pacific SST. Measured by ΔT in Eq. (2), the equatorial zonal SST contrast in the absence of ocean–atmosphere coupling is increased by 0.27°C. This increase is small, but significant. Once the equatorial zonal wind stress is coupled to the zonal SST gradients via Eq. (2), this initial cooling to the eastern Pacific SST is amplified: stronger winds result in stronger upwelling which in turn strengthens the zonal SST contrast. As shown in Fig. 2a, the zonal SST contrast in the cold period of the coupled case is increased by as much as 1.9°C. Therefore, the subtropical cooling impinges on the stability of the coupled equatorial Pacific ocean–atmosphere system via its effect on the difference between T_w and T_c and then on the equatorial zonal SST contrast. The effect on the latter involves the coupling between the atmosphere and ocean. Apparently, the onset of a regime with stronger ENSO is a coupled response to this destabilizing tendency. Extending this reasoning, one expects that the ENSO may act as a stabilizer of the coupled equatorial Pacific ocean–atmosphere system: the presence of ENSO may reduce the sensitivity of $T_w - T_c$ in the mean state to an external forcing.

Indeed, once the coupling is turned on and ENSO is allowed to develop, the enhanced subtropical cooling has a much reduced impact on the difference between T_w and T_c in the time-mean state. Comparing Fig. 5 with Fig. 2c, it reveals that the change in the time-mean

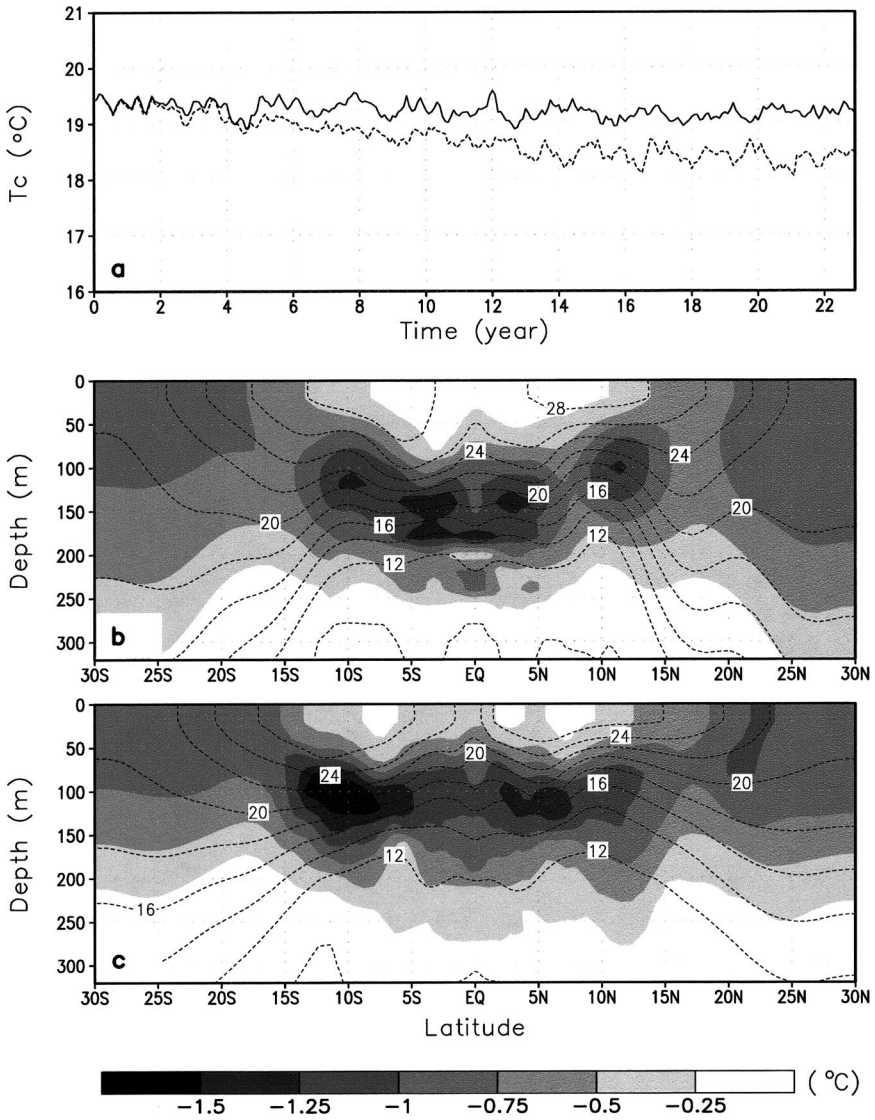

FIG. 4. (a) Time series of the core temperature of the equatorial undercurrent (T_c) from two uncoupled runs. The control run corresponds to the solid line, and the perturbed run corresponds to the dashed line. The form of cooling for the perturbed run is the same as for the coupled perturbed run (Fig. 1b). The value of T_c is obtained by first finding for all longitudes the equatorial ocean temperature at the depth where the zonal velocity has its maximum, and then zonally averaging this temperature from 180° to 270°E. (b), (c) Meridional cross sections of the upper-ocean temperature difference in the central (160°–210°E) and eastern Pacific (210°–270°E) during the last 3 yr of the run. The thin dashed contours indicate the mean isentropes of the control run.

temperature of the equatorial thermocline water in the coupled case is less than half of that in the uncoupled case. (The cooling to T_c is reduced from about 0.85° to 0.32°C). Also, ENSO causes significant cooling to the SST of the western Pacific warm pool. (In the coupled case T_w is cooled by 0.79°C compared to a negligible 0.04°C in the uncoupled case.) Consequently, the time-mean difference between the warm-pool SST and the temperature of the equatorial thermocline water induced by the imposed subtropical cooling in the coupled case (Fig. 2c) is much reduced compared to that in the corresponding uncoupled case (Fig. 5). The lack of change in the time-mean difference between the warm-pool SST and the temperature of the equatorial themocline water also prevents significant change from occurring in the time-mean equatorial zonal SST contrast. Measured by the value of ΔT in Eq. (2), the change in the time-mean zonal SST contrast is a negligible 0.025°C. The apparent lack of sensitivity in the time-mean zonal SST contrast even in the presence of the positive Bjerknes feedback is also linked to the fact that the enhanced subtropical/extratropical cooling apparently mainly cools the cold

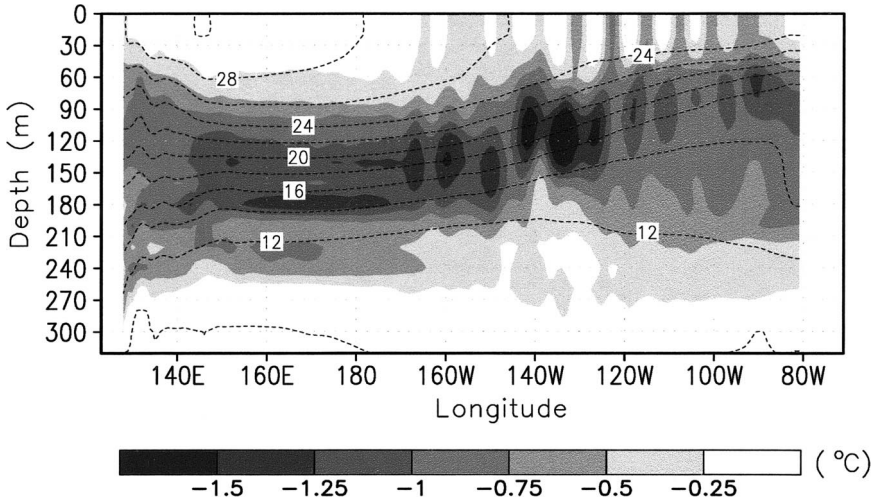

FIG. 5. The temperature differences in the equatorial upper ocean (5°S–5°N) between the uncoupled control run and the corresponding uncoupled perturbed run described in Figs. 4b,c. As for those figures, the last 3 yr of a 23-yr-long run are used in the calculation.

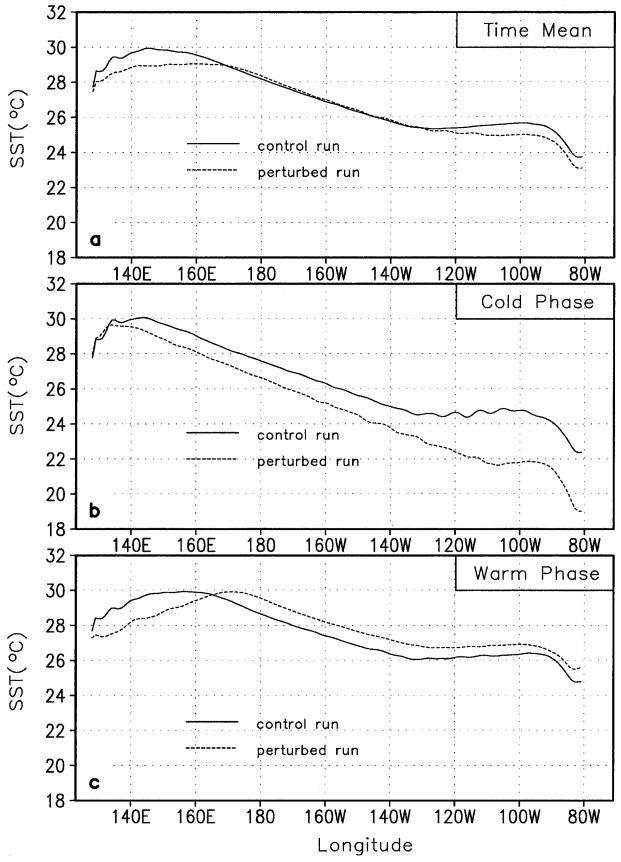

FIG. 6. Zonal distribution of the equatorial SST (5°S–5°N) for the control run (solid line) and the perturbed run (dashed line) (a) in the time mean, (b) during the cold phase, and (c) during the warm phase.

phase of ENSO in the equatorial region east of the date line (Fig. 6b). But then El Niño events are stronger, which largely reverses the cooling effect during the cold phase (Fig. 6c). This cancellation effect is evident in Fig. 2.

Detailed examination of the coupled perturbed run reveals that the onset of the regime with stronger ENSO is triggered when the equatorial thermocline water is cooled significantly and when this cooling coincides with an ongoing La Niña event. Figure 7 shows the time series of the temperature of the equatorial undercurrent (T_c) for the coupled control run and the corresponding perturbed run. A significant cooling to T_c occurred at about the 44th month, but this cooling is short-lived. This cooling may indicate the passage of the first packet of waves. A persistent difference between the T_c in the perturbed run and the T_c in the control run starts to occur at about the 55th month. This is followed by a significant

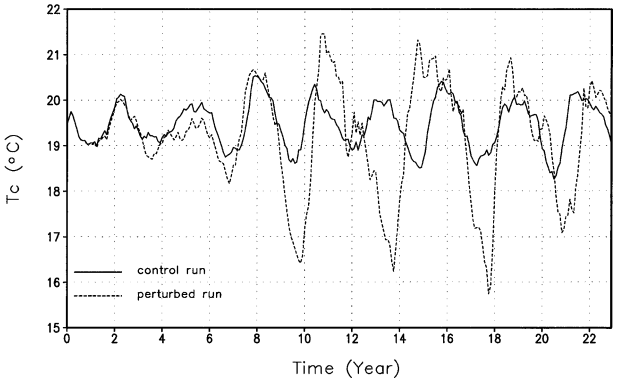

FIG. 7. Time series of the core temperature of the equatorial undercurrent (T_c) from the coupled control run (solid line) and the corresponding perturbed run (dashed line). The value of T_c is obtained the same way as in Fig. 4a.

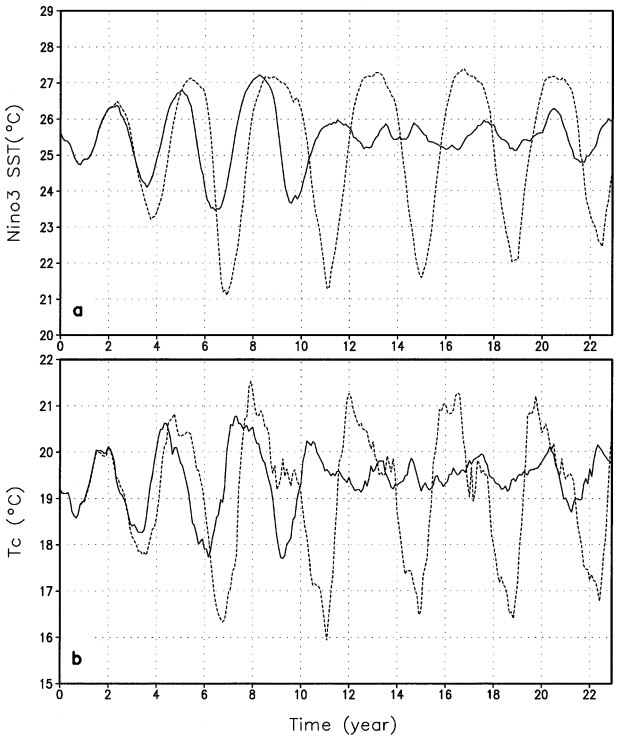

FIG. 8. Time series of (a) Niño-3 SST and (b) T_c from another pair of coupled runs—a control run (solid line) and a perturbed run (dashed line). This pair of runs is the same as the pair shown in Figs. 1 and 7 except in the initial conditions from which the runs start. The value of T_c is calculated the same way as in Fig. 4a.

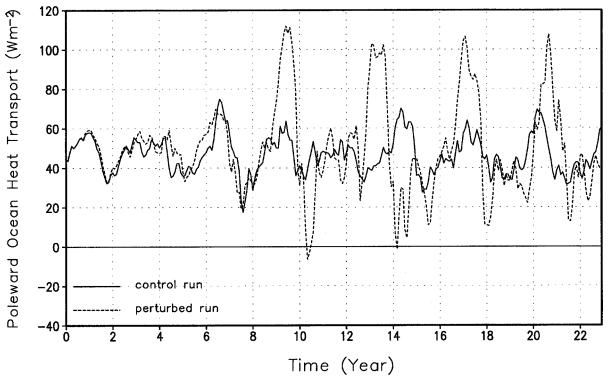

FIG. 9. Time series of the poleward heat transport out of the equatorial Pacific (5°S–5°N) from the control run (solid line) and the perturbed run (dashed line).

difference between the Niño-3 SST in the perturbed run and the control run about 5 months later (see Fig. 1a). This initial cooling happens to be in a growth phase of El Niño. This El Niño is therefore damped. The subsequent La Niña is, however, strengthened by this cooling. After this stronger La Niña, El Niño becomes warmer, apparently because of the coupling. A regime with stronger ENSO then develops.

To confirm the order of this sequence of events, we have run another pair of experiments—a coupled control run and a corresponding perturbed run. The Niño-3 SST and T_c from these two runs are shown in Fig. 8. This pair of runs only differs from the previous pair in the initial conditions from which the integration starts. Again, the imposed surface cooling triggers the onset of a regime with stronger ENSO at the time when its cooling effect on the equatorial thermocline coincides with an ongoing La Niña. Note also that T_c generally leads the Niño-3 SST though the lead varies (2–8 months); T_c is anomalously warm prior to the onset of the warm events and anomalously cold prior to the onset of the cold events.

El Niño in this model results from a coupled instability. The reason that a stronger El Niño develops after a stronger La Niña is because a stronger La Niña pumps more heat down to the subsurface ocean of the equatorial western Pacific and renders the coupled system more unstable (Fig. 2a). ENSO in this model behaves like a pendulum: if you push the pendulum to the direction where it is already swinging into, it will be able to climb higher when it swings back.

A stronger El Niño results in stronger poleward heat transport. Figure 9 shows the time series of the poleward heat transport away from the equatorial Pacific from the control run and the perturbed run. Comparing with Fig. 1, it shows that the poleward heat transport lags the surface warming: as the surface warming reaches its peak, the equatorial Pacific continues to lose more heat to the higher latitudes, pushing the equatorial Pacific to a La Niña state. This lag between the surface warming and the poleward heat transport therefore acts as a phase transition mechanism.

Figures 1 and 8 also show that in response to the subtropical cooling, the period of the oscillation becomes longer. This reduction in the frequency of ENSO is probably linked to the increase in the amplitude of ENSO. As originally found in the model of Zebiak and Cane (1987) and further delineated in the weakly nonlinear analysis of Jin (1997), a stronger oscillation tends to be accompanied by a reduced frequency—a longer period. Detailed analysis of factors that influence the frequency of ENSO in the present model will be presented in a later paper.

The sensitivity of ENSO in the model to the subtropical cooling appears to be high. The cooling to the equatorial thermocline water is about 1.0°C (Figs. 4 and 5). The change in the amplitude of ENSO is from about 2° to about 6°C: the Niño-3 SST at the peak of the La Niña phase is about 3.5°C cooler while the Niño-3 SST at the peak of the El Niño phase is about 0.5°C warmer (Fig. 1a). The amplification of the cooling during the La Niña phase is due to the Bjerknes feedback—the positive feedback loop between the equatorial zonal SST gradients, the equatorial zonal wind stress, and the equatorial upwelling. An initial cooling to the eastern equatorial Pacific SST due to the upwelling of the colder equatorial thermocline water causes a strengthening of the zonal SST contrast and thereby a strengthening of

the zonal winds. The slightly stronger El Niño is a simple response to the stronger La Niña as the two phases of ENSO involve a zonal redistribution of the heat in the equatorial upper ocean. Therefore, the sensitivity of ENSO to the subtropical cooling depends on the strength of the Bjerknes feedback. The strength of the Bjerknes feedback is measured by the coupling strength parameter μ. As mentioned before, our estimate of μ is based on the NCEP reanalysis and therefore is only realistic to the degree that the NCEP wind stress is realistic. In addition, the coupling between the winds and the SST in the present model is also idealized. It is possible that in a more sophisticated model, the sensitivity of ENSO to subtropical cooling is weaker. On the other hand, we have to note that the imposed cooling is not small—it is certainly larger than observed changes in the subtropical Pacific temperature on decadal time scales. For example, the maximum difference in the extratropical Pacific SST between the epoch 1977–93 and the preceding epoch 1950–76 is less than 0.5°C (Zhang et al. 1997).

We have further verified that the delay in the response of ENSO to a subtropical/extratropical cooling become progressively longer as we move the cooling progressively to the higher latitudes. An example is shown in Fig. 10. Now the onset of a regime with stronger ENSO does not occur until almost 12 yr later.

We have also found that the cooling outside the region of 20°S–20°N contributes to most of the response of ENSO in Fig. 1. Figures 11a and 11b show, respectively, the response of Niño-3 SST to the surface cooling shown in Figs. 11c and 11d. The surface cooling used for Fig. 1 is now divided into two parts. Cooling shown in Fig. 11d is confined to the region poleward 20°. Figure 11c shows the remaining part of the cooling. The initial response in the Niño-3 SST variability shown in Fig. 1a is apparently due to the cooling in the region of 5°N(S)–20°N(S), but the influence of cooling from this region on the Niño-3 SST is weak and is dampened after 10 yr of its arrival. The response in amplitude due to the cooling in Fig. 11d is very close to the response to the total cooling shown in Fig. 1. This is because the cooling to the equatorial thermocline water shown in Fig. 5 is mainly due to the surface cooling imposed in the region poleward of 20°S–20°N. Figures 12a and 12b show, respectively, the effect of the surface cooling shown in Figs. 11c and 11d on the equatorial thermocline temperature.

We have also done experiments with the surface cooling replaced by surface warming. With sufficiently strong subtropical warming, ENSO can be killed entirely (Fig. 13). This result is expected from the cooling experiments. While subtropical cooling tends to destabilize the equatorial ocean–atmosphere system through reducing the temperature of the equatorial thermocline water, the subtropical heating tends to stabilize the equatorial ocean–atmosphere system by warming up the equatorial thermocline water. The warming effect of the surface heating shown in Fig. 13b on the equatorial thermocline water is shown in Fig. 14. To isolate the stabilizing effect of the subtropical heating on the equatorial ocean–atmosphere system, the equatorial ocean–atmosphere coupling is again turned off in obtaining Fig. 14. The figure shows a substantial reduction in the value of $T_w - T_c$ (~1.6°C) and a substantial reduction in the value of ΔT (~0.56°C). Consequently, the equatorial ocean–atmosphere system is completely stabilized.

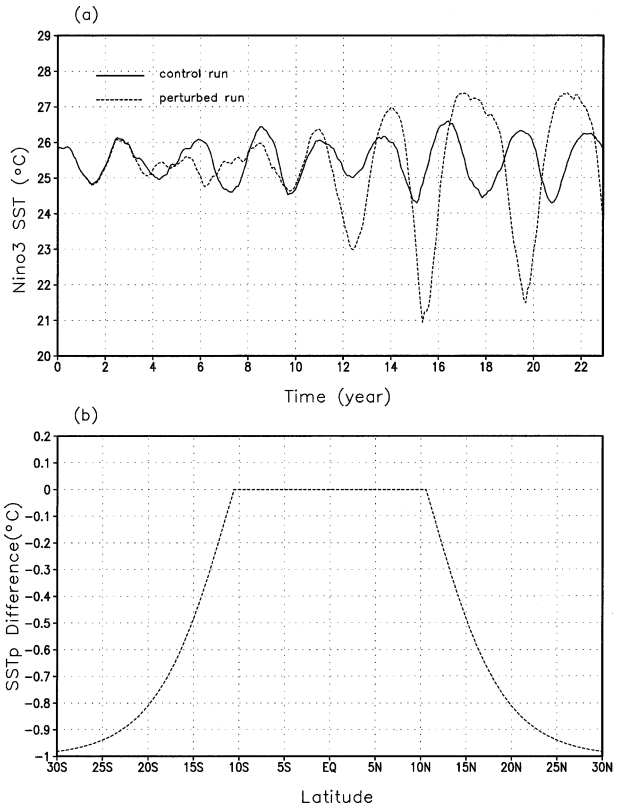

FIG. 10. (a) Time series of Niño-3 SST from a control run (solid line) and a perturbed run (dashed line). The control run is the same as shown in Fig. 1a. (b) The reduction in SST_p the perturbed run shown here is subjected to. The cooling starts from a higher latitude than that in Fig. 1b, and due to the higher latitude, there is a prolonged delay in the response of the Niño-3 SST.

The domain of the present model prevents us from moving the surface cooling beyond regions poleward of 30°N or 30°S. As we remarked before, the ideal setting to test the heat-pump hypothesis is to impose a cooling that centers about the latitude where the 20°C isotherms outcrop. For the observed annual mean situation, this latitude is about 35°N in the North Pacific and 30°S in the South Pacific. This is why we maximize the cooling near the model boundary in the present model setting. We are also helped by the fact that surface cooling imposed in the subtropical region sinks locally to considerable depth (Figs. 4b,c). Provided that surface cooling in these regions induces upper-ocean temperature differences within the tropical domain similar to those

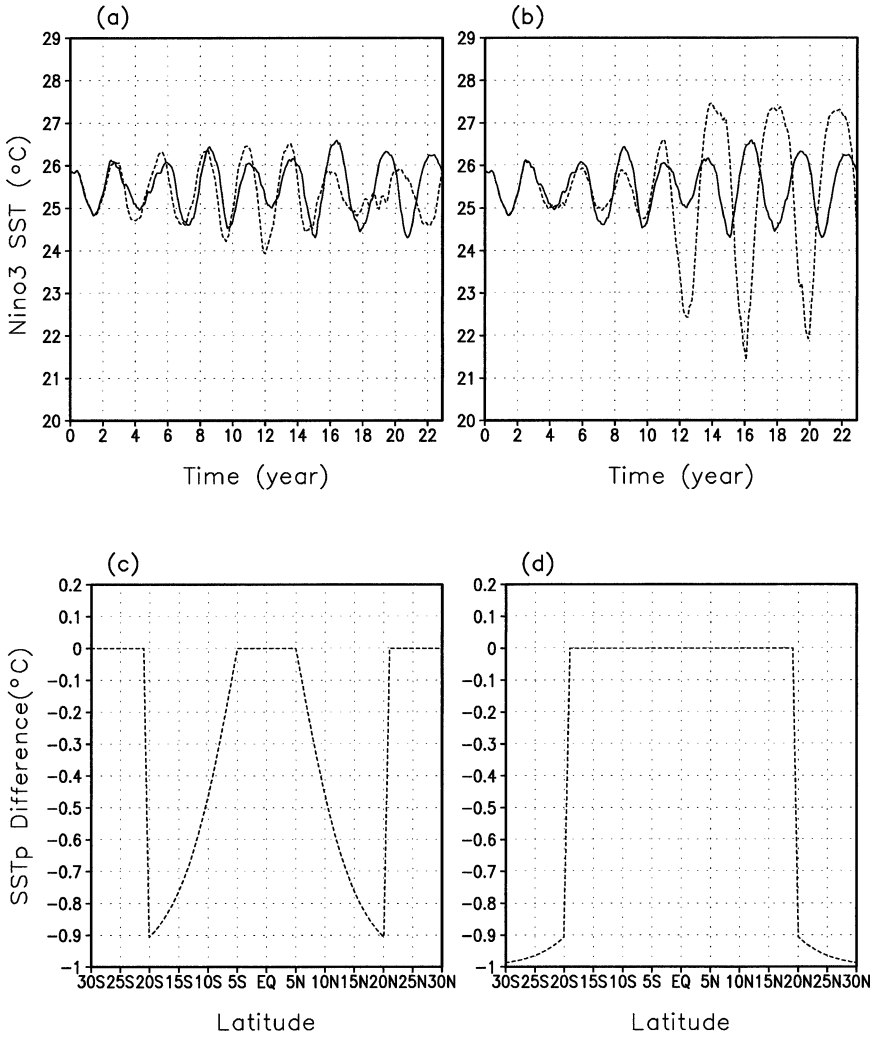

FIG. 11. (a) Response of Niño-3 SST to cooling in the form shown in (c). (b) Response of Niño-3 SST to cooling in the form shown in (d). Note that the sum of (c) and (d) equals the cooling shown in Fig. 1b.

shown in Figs. 4b,c and Fig. 5, we do not expect any qualitative difference in the effect of a midlatitude cooling on ENSO from the experiments we have reported here. Therefore, the cooling from the higher latitudes via subduction may be partially simulated here.

A related question is whether ENSO will still respond the same way when surface cooling is imposed in the very high latitudes where the intermediate water and deep water originate. Considering that such a cooling will ultimately affect the equatorial deep-ocean temperature via the global thermohaline circulation (Broecker 1987), Sun (2000) suggests a positive impact of such a cooling on ENSO, citing results from a highly idealized model. By simply reducing the equatorial deep-ocean temperature in the present model, we find that a cooling in the deep-ocean temperature in this model indeed results in a regime of stronger ENSO (Fig. 15). While this result supports the speculation by Sun (2000), it should be viewed with caution as the ocean model used in this study was mainly designed as an upper-ocean model, and the communication between the equatorial deep ocean and the equatorial upper ocean in this model is not realistic. For example, a reduction in the deep-ocean temperature in the present model is immediately felt by the upper ocean overlying it via entrainment (Gent and Cane 1989). This treatment may not simulate the actual upwelling from the deep ocean.

4. Conclusions

Numerical experiments have been conducted to investigate the effect of an enhanced subtropical surface cooling on the level of ENSO activity. The results show that such a perturbation to the surface heating can indeed result in a regime with stronger ENSO activity. Moreover, ENSO appears to regulate the time-mean differ-

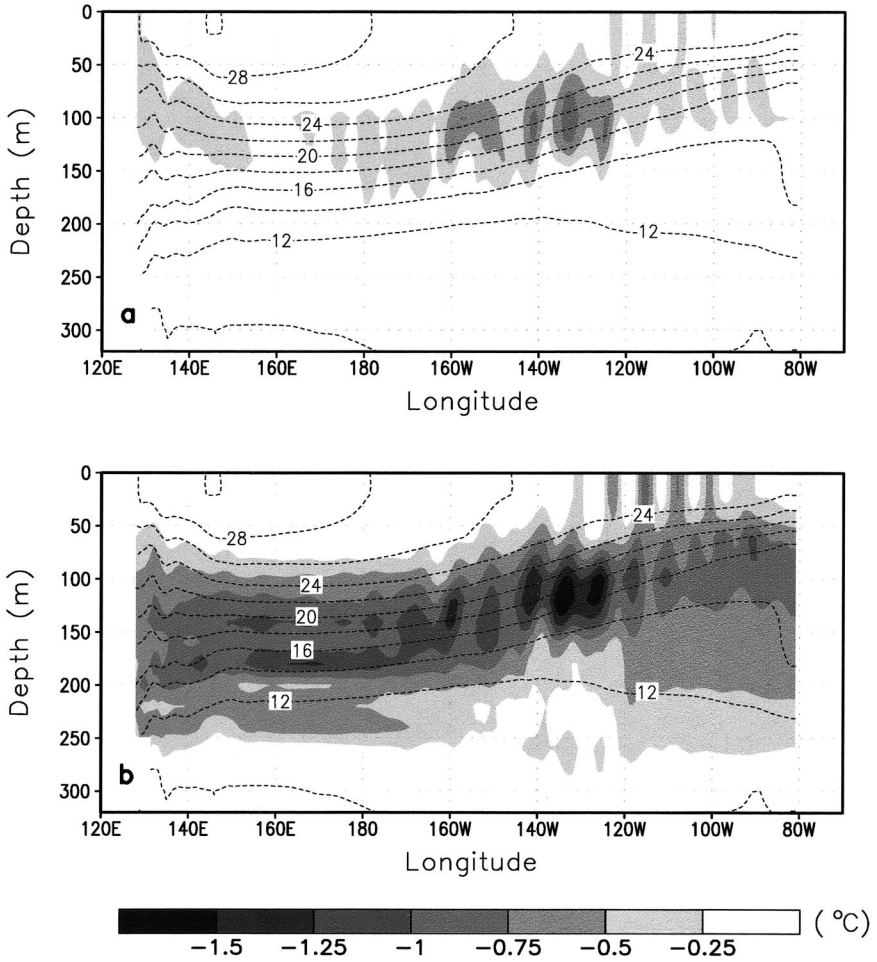

FIG. 12. (a), (b) The cooling to the equatorial thermocline water due to the cooling shown in Figs. 11c and 11d, respectively. Shown are the upper-ocean temperature differences in the equatorial region (5°S–5°N) between an uncoupled control run and the corresponding uncoupled perturbed run. Both runs are 23 yr long. The last 3 yr of the runs are used for this calculation. The dashed contours indicate the mean isentropes of the control run.

ence between the warm-pool SST (T_w) and the temperature of the equatorial undercurrent (T_c).

The enhanced subtropical surface cooling influences the level of ENSO through cooling the equatorial undercurrent and the associated equatorial upwelling water. With the radiative–convective equilibrium SST over the equatorial region being kept fixed, the difference between the warm-pool SST (T_w) and the temperature of the equatorial undercurrent (T_c) tends to become larger. This tendency constitutes a destabilizing effect on the stability of the coupled equatorial ocean–atmosphere system. A regime with stronger ENSO develops apparently as a coupled response to this destabilizing forcing. While the enhanced subtropical cooling is found to induce a substantial increase in the difference between T_w and T_c in the absence of ENSO, it results in little increase in the time-mean difference between T_w and T_c in the presence of ENSO. This contrast in the response to the enhanced subtropical cooling provides evidence that ENSO regulates the long-term stability of the coupled equatorial ocean–atmosphere system.

The findings here are consistent with the argument presented in Sun (2003): El Niño corresponds to a poleward heat transport mechanism. Either an increase in the equatorial surface heating or an increase in the subtropical/extratropical cooling should result in a regime with more energetic ENSO events. Moreover, ENSO may be a mechanism that regulates the long-term stability of the coupled equatorial ocean–atmosphere system. In addition, the present findings appear to substantiate the argument of Gu and Philander (1997) and Zhang et al. (1998) that the ''ocean tunnel'' may be an important mechanism for decadal variability.

Surface thermal forcing in the subtropical/extratropical region may affect equatorial SST variability through many pathways. The present study focuses on the role of the ocean tunnel. Correspondingly, the experiments reported here are highly idealized. The winds and SST

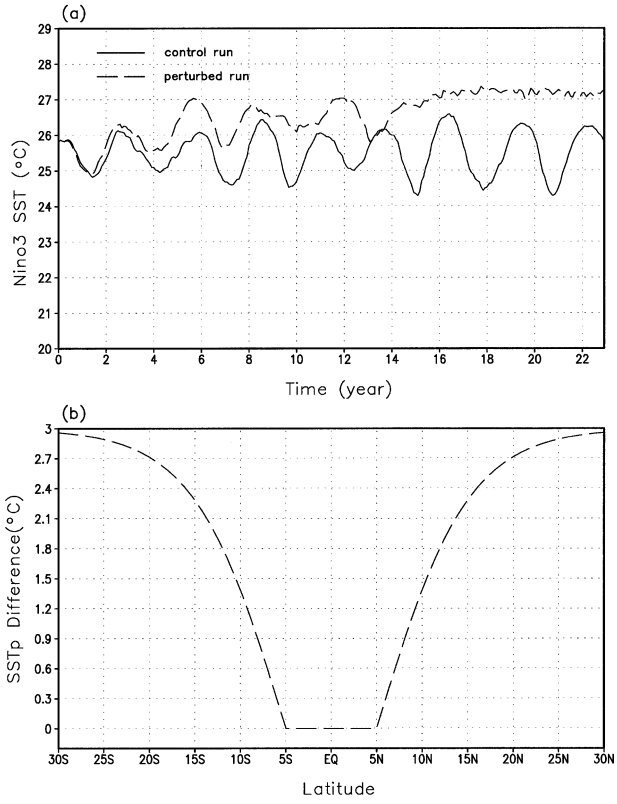

FIG. 13. (a) Response of Niño-3 SST to subtropical heating. The solid line is for the control run. The dashed line is for the perturbed run. (b) The subtropical heating imposed in the perturbed run.

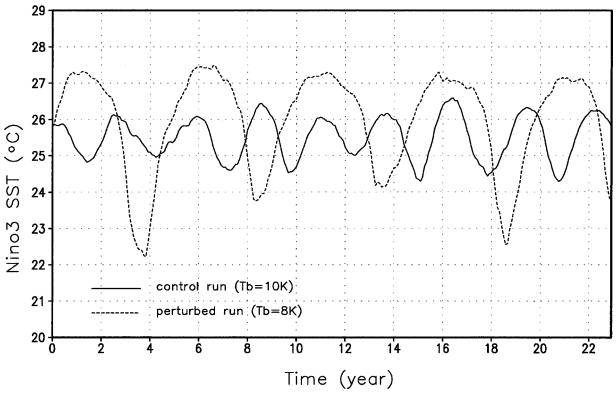

FIG. 15. Time series of Niño-3 SST from a control run (solid line) and a perturbed run (dashed line). The control run is the same as in Fig. 1a. The perturbed run has a colder deep-ocean temperature—2 K colder than in the control run. Recall that in this model, there is only one temperature for the deep ocean—the part of the ocean that does not feel the wind forcing and is motionless. The deep-ocean temperature, however, affects the upper-ocean temperature by entrainment (Gent and Cane 1989).

are only coupled in the equatorial region. Presumably, as the subtropical/extratropical ocean cools, the Hadley circulation may become stronger and the subtropical/extratropical surface winds may change correspondingly. These changes may in turn influence the equatorial SST response. This model also lacks a seasonal cycle and the associated monsoonal circulation, both of which have been hypothesized as important players in projecting the influence of a global forcing over ENSO (Clement et al. 2000; Liu et al. 2000). Our next step is to couple the present ocean model with a global atmosphere so that the feedbacks from the global atmo-

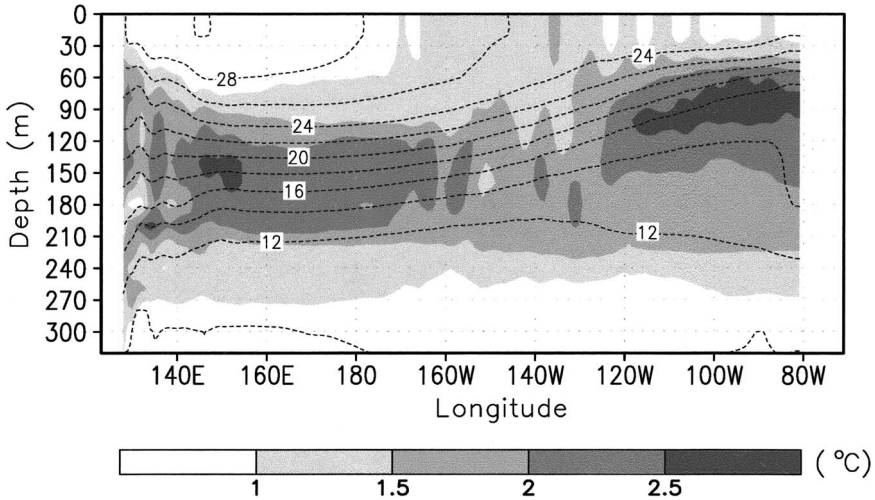

FIG. 14. The equatorial upper temperature differences (5°S–5°N) induced by the subtropical heating shown in Fig. 13b. Shown are the mean differences between an uncoupled control run and an uncoupled perturbed run over the last 3 yr of a 23-yr-long run. Note the significant reduction in the difference between western Pacific warm-pool SST and the temperature of the thermocline water ($T_w - T_c$) and the corresponding reduction in the zonal SST contrast (ΔT) between the equatorial western Pacific and the equatorial eastern Pacific.

spheric circulations could be better represented. The present results should be useful for understanding results from more complicated models, such as those from a recent study by Otto-Bliesner et al. (2003) using NCAR Climate System Model (CSM).

Additional experiments with a global ocean model are also needed. A global ocean model allows us to examine more carefully the response of ENSO to enhanced cooling in the region poleward of 30°N and 30°S including cooling in other basins. A global ocean model may also reveal a role of the global thermohaline circulation in linking ENSO to the high-latitude surface conditions. All these details may potentially modify the mechanism suggested here by which subtropical/extratropical cooling affects ENSO. Nonetheless, the present experiments are potentially valuable as a stepping stone for a more complete understanding and assessment of the role of the ocean tunnel in linking the high-latitude surface forcing to the behavior of ENSO on decadal and longer time scales.

The ultimate test of the mechanism by which a subtropical/extratropical cooling on ENSO and the heat-pump hypothesis for ENSO in general has to come from observations, paleoclimate observations in particular. In this connection, it may be worth noting the recent data from Cobb et al. (2003). Her coral records appear to suggest that ENSO during the Little Ice Age (LIA) was stronger than in the Medieval Warm Period (MWP). She has also noted in the same record that the time-mean tropical climate has little change from periods of weak ENSO activity to periods of strong ENSO activity. The present findings concerning the regulatory effect of ENSO on the tropical mean climate suggest that the lack of change in the local time-mean state (i.e., the mean tropical Pacific climate) may be precisely due to the large variations in the level of ENSO activity. Chaos and weather noise within the Tropics may play a significant role in the variability of ENSO on decadal and longer time scales. But the present results suggest that in order to identify all the causes for the variability of ENSO on decadal and longer time scales, one may have to keep in mind the role of the ocean tunnel and look beyond the tropical Pacific and look poleward.

Acknowledgments. This research was partially supported by the NSF Climate Dynamics Program (ATM-9912434) and partially by NOAA's Office of Global Programs (the CLIVAR/Pacific Program, the CLIVAR PACS Program, and the Climate Dynamics and Experimental Prediction Program). Computing support was provided by NCAR SCD. The authors would like to thank Dr. Xiangze Jin for his help in the early stage of the work. The authors would also like to thank Drs. Mark Cane, Peter Gent, Julian McCreary, and Paul Schopf for the helpful discussions, and the two anonymous reviewers for their helpful comments.

REFERENCES

Alexander, M. A., I. Bladé, M. Newman, J. R. Lanzante, N.-C. Lau, and J. D. Scott, 2002: The atmospheric bridge: The influence of ENSO teleconnections on air–sea interaction over the global oceans. *J. Climate,* **15,** 2205–2231.

Broecker, W. S., 1987: The biggest chill. *Natural History Magazine,* October, 74–82.

Clement, A. C., R. Seager, and M. A. Cane, 2000: Suppression of El Niño during the mid-Holocene by changes in the Earth's orbit. *Paleoceanography,* **15,** 731–737.

Cobb, K. M., C. D. Charles, H. Cheng, and R. L. Edwards, 2003: El Niño/Southern Oscillation and tropical Pacific climate during the last millennium. *Nature,* **424,** 271–276.

Galanti, E., and E. Tziperman, 2003: A midlatitude–ENSO teleconnection mechanism via baroclinically unstable long Rossby waves. *J. Phys. Oceanogr.,* **33,** 1877–1888.

Gent, P. R., 1991: The heat budget of the TOGA-COARE domain in an ocean model. *J. Geophys. Res.,* **96,** 3323–3330.

——, and M. A. Cane, 1989: A reduced gravity, primitive equation model of the upper equatorial ocean. *J. Comput. Phys.,* **81,** 444–480.

Gu, D.-F., and S. G. H. Philander, 1997: Interdecadal climate fluctuations that depend on exchanges between the Tropics and extratropics. *Science,* **275,** 805–807.

Jin, F.-F., 1996: Tropical ocean–atmosphere interaction, the Pacific cold-tongue, and the El Niño–Southern Oscillation. *Science,* **274,** 76–78.

——, 1997: An equatorial ocean recharge paradigm for ENSO. Part II: A stripped-down coupled model. *J. Atmos. Sci.,* **54,** 811–829.

Kalnay, E., and Coauthors, 1996: The NCEP/NCAR 40-Year Reanalysis Project. *Bull. Amer. Meteor. Soc.,* **77,** 437–471.

Liu, Z., and S.-I. Shin, 1999: On the thermocline ventilation of active and passive tracers. *Geophys. Res. Lett.,* **26,** 357–360.

——, S. G. H. Philander, and P. C. Pacanowski, 1994: A GCM study of tropical–subtropical upper-ocean water exchange. *J. Phys. Oceanogr.,* **24,** 2606–2623.

——, J. Kutzbach, and L. Wu, 2000: Modeling climatic shift of El Niño variability in the Holocene. *Geophys. Res. Lett.,* **27,** 2265–2268.

Lu, P., J. P. McCreary, and B. A. Klinger, 1998: Meridional circulation cells and the source waters of the Pacific equatorial undercurrent. *J. Phys. Oceanogr.,* **28,** 62–84.

McCreary, J. P., Jr., and P. Lu, 1994: Interaction between the subtropical and equatorial ocean circulations: The subtropical cell. *J. Phys. Oceanogr.,* **24,** 466–497.

Neelin, J. D., D. S. Battisti, A. C. Hirst, F.-F. Jin, Y. Wakata, T. Yamagata, and S. Zebiak, 1998: ENSO theory. *J. Geophys. Res.,* **103,** 14 261–14 290.

Otto-Bliesner, B. L., E. C. Brady, S.-I. Shin, Z. Liu, and C. Shields, 2003: Modeling El Niño and its tropical teleconnections during the last glacial–interglacial cycle. *Geophys. Res. Lett.,* **30,** 2198, doi:10.1029/2003GL018553.

Pedlosky, J., 1987: An inertial theory of the equatorial undercurrent. *J. Phys. Oceanogr.,* **17,** 1978–1985.

Rayner, N. A., E. B. Horton, D. E. Parker, C. K. Folland, and R. B. Hackett, 1996: Version 2.2 of the global sea-ice and sea surface temperature data set, 1903–1994. Climate Research Tech. Note CRTN74, Hadley Centre for Climate Prediction and Research, Met Office, United Kingdom, 35 pp.

Schneider, N., A. J. Miller, M. A. Alexander, and C. Deser, 1999: Subduction of decadal North Pacific temperature anomalies: Observations and dynamics. *J. Phys. Oceanogr.,* **29,** 1056–1070.

Shin, S.-I., and Z. Liu, 2000: Response of the equatorial thermocline to extratropical buoyancy forcing. *J. Phys. Oceanogr.,* **30,** 2883–2905.

Sun, D.-Z., 1997: El Niño: A coupled response to radiative heating? *Geophys. Res. Lett.,* **24,** 2031–2034.

——, 2000: Global climate change and ENSO: A theoretical framework. *El Niño: Historical and Paleoclimatic Aspects of the*

Southern Oscillation, Multiscale Variability and Global and Regional Impacts, H. F. Diaz and V. Markgraf, Eds., Cambridge University Press, 443–463.

——, 2003: A possible effect of an increase in the warm-pool SST on the magnitude of El Niño warming. *J. Climate,* **16,** 185–205.

——, and Z. Liu, 1996: Dynamic ocean–atmosphere coupling: A thermostat for the Tropics. *Science,* **272,** 1148–1150.

Trenberth, K. E., G. W. Branstator, D. Karoly, A. Kumar, N.-C. Lau, and C. Ropelewski, 1998: Progress during TOGA in understanding and modeling global teleconnections associated with tropical sea surface temperatures. *J. Geophys. Res.,* **103,** 14 291–14 324.

Zebiak, S. E., and M. A. Cane, 1987: A model El Niño–Southern Oscillation. *Mon. Wea. Rev.,* **115,** 2262–2278.

Zhang, R.-H., L. M. Rothstein, and A. J. Busalacchi, 1998: Origin of upper-ocean warming and El Niño change on decadal scales in the tropical Pacific Ocean. *Nature,* **391,** 879–883.

Zhang, Y., J. M. Wallace, and D. S. Battisti, 1997: ENSO-like interdecadal variability. *J. Climate,* **10,** 1004–1020.